SUPERELASTIC LIGHTWEIGHT CARBON MATERIALS FOR PIEZORESISTIVE SENSORS

Irina PLEȘCO

National Center for Materials Study and Testing, Technical University of Moldova

***Abstract**. This article aims to give a comparative overview on carbonic materials of various geometries and compositions, which are developed for applications in production of strain and pressure sensors. We discuss the preparation methods and resulting geometries of carbonic porous materials, hybrid and reinforced composites. Various architectures combined with synergistic effect of graphene and additional components reveal a series of mechanical properties (compressibility, fatigue resistance, time of recovery) and variation of electrical parameters, which make them suitable for integration in wearable electronics as highly sensitive devices.*

Presented materials refer to own investigations and published studies of other research groups.

***Key words:** graphene aerogel; strain sensor; pressure sensor;piezorezistive sensor.*

Introduction

Strain and pressure sensors represent one of the most popular research topics in recent years. Light flexible sensors can become base components for wearable personal electronics. Carbon and graphene materials of all possible geometries have been developed recently [1-3]. They compete in electrical conductivity, mechanical hardness and flexibility, density and production cost. These materials provide great potential for applications in mechatronics, robotics, automation, human-machine interaction, etc. In order to mount easier the wearable sensors on the human skin for real-time human motion detection, several performance and parameter requirements need to be fulfilled. Lightweight, flexibility, stretchability, durability, biocompatibility, and low power consumption are crucial properties for wearable sensors [4-6].

Transduction methods of graphene-based strain and pressure sensors include resistive [7, 8], capacitance [9, 10], and piezoelectricity [11-12].

Resistive sensors convert external forces into a variation of resistance, which can be directly detected through changes in the electrical signals. It obtains a resistive sensing signal through the change of the resistance [12-15]. Due to a simple measurement method and the large scope of applications [16], resistive sensors have been widely used. Resistive effect is generated by an applied external force changing the conductive path of the sensing material, which changes the resistance. Piezorezistive effect was found in single layer CVD graphene [17] and was demonstrated by construction of a graphene-membrane pressure sensor. At the same time effect didn't depend on cristallographic alignment of the layer and multiple grain flakes. It means, that the piezoresistive effect can manifest both in single layers as well as in multi-layered structures like graphene aerogel. Piezorezistive effect consists in change of electrical resistance under applied pressure. As a common type of strain and pressure sensor, the advantages of graphene-based resistive sensors are a wide detection range, simple equipment construction, and signal testing.

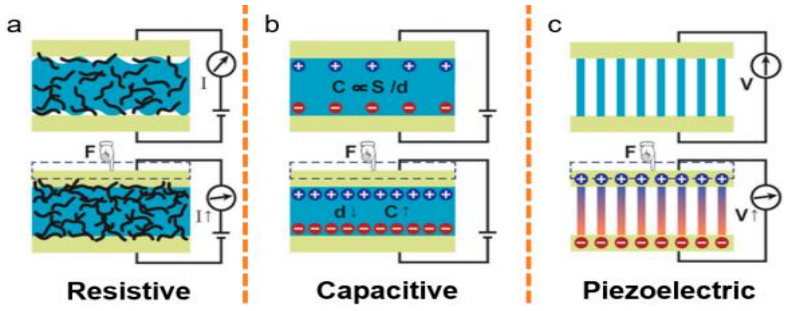

Fig. 1. Schematics of different sensing mechanisms of graphene strain and pressure sensors. Copyright 2018 Elsevier Ltd. [18].

Another sensing mechanism is represented by capacitive strain and pressure sensors [19-22]. The base principle consist in conversion of mechanical displacement into capacitance change. Force variation in different directions is detected by changes of sensor's effective area and the spacing between contacts to obtain an electrical signal [23]. Capacitive sensors exhibit extreme sensitivity to weak changes and are suitable for detection of small forces [24-26].

Major Parameters of Graphene-Based Strain and Pressure Sensors

The sensitivity of pressure sensors generally refers to the ratio between the variables involved in the output and input signals. For graphene-based pressure sensors with different transduction mechanisms, the input and output signals are different. For instance, the sensitivity of resistive pressure sensors is calculated by dividing the relevant variation of resistance by the variation of the applied pressure. In the same way, sensitivities of capacitive and piezoelectric pressure sensors correspond to capacitance and voltage, respectively

$$S = \left|\frac{\Delta R/R_0}{\Delta P}\right| \quad (1)$$

Gauge factor, which makes no sense to pressure sensors, is an important parameter for strain sensors. Gauge factor (GF), also named strain factor, of a strain sensor is the ratio of the relevant change in electrical resistance R, to the mechanical strain ε, which means this parameter is only significant for the resistive strain sensor

$$GF = \left|\frac{\Delta R/R_0}{\varepsilon}\right| \quad (2)$$

Linearity is an important indicator to describe the static characteristics of a sensor. It is used to characterize the parameters whose actual characteristics do not match the fitted line. In certain conditions, the ratio of the maximum deviation between the sensor calibration curve to the fitted line and the full-scale output is called linearity, also known as nonlinearity error [27]. For the graphene-based strain and pressure sensors, it is still a technical challenge to balance the relationship between sensitivity and linearity. At present, researchers still cannot achieve both high sensitivity and good linearity for graphene-based strain and pressure sensors, which needs further study.

Hysteresis is another important indicator of sensor performance. Hysteresys of stress-strain or strain-resistance curves between forward and backward cycling is observed due to the fact that, when the sensor is compressed and released, graphene flakes require a specific amount of time to return to their original position. Effect of hysteresis shows how high is mechanical instability or damage of sensor. Hence, hysteresis is an important parameter for graphene-based strain and pressure sensors.

Piezorezistive 3D graphene aerogel/semiconductor pressure sensors

Hybrid graphene aerogel/semiconductor structures for pressure sensor fabrication were prepared by magnetron sputtering of nanocrystalline layers of semiconductors on graphene aerogel substrates acquired from Graphene Supermarket.

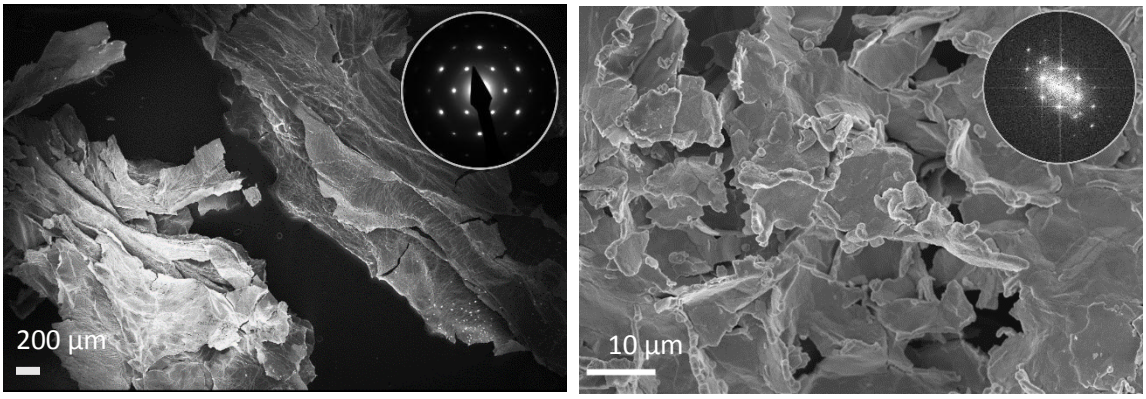

Fig. 2. SEM images of pure graphene aerogel (left) and aerogel/CdS hybrid structure, insets show diffraction patterns confirming high crystallinity of graphene and CdS.

Our previous investigations disclosed the presence of individual well exfoliated graphene nano-sheets in the GA specimens [11, 12]. The CdS, InP, CdTe and GaN nanocrystalline films were deposited on graphene aerogel by RF magnetron sputtering techniques in a high vacuum chamber. Distance between electrodes was set at 8 cm, the pressure in chamber was maintained at 7.4×10^{-3} mbar, was maintained Ar flow at 60 ml min^{-1}. MTM-10/10 A High Resolution thickness monitor quartz microbalance was used to

control the film thickness during sputtering. CdS, InP, CdTe and GaN wafers served as targets for sputtering. The substrate temperature (Ts), kept at 30 °C, was controlled by using a chromel-alumel thermocouple.

The high crystalline quality of the graphene aerogel is demonstrated by the diffraction pattern analysis (Fig. 2 insets). The disclosed crystalline phase of semiconductor layers corresponds to wurztite type $P6_3mc$. Lattice parameters of nanocrystal are slightly increased. This might have its origin in the intergrowth with the aerogel substrate. The promising pressure sensing properties are attributed to the large surface to volume ratio and accordingly large area exposed to pressure differentials. This in turn makes the entirety of the piezoelectric component susceptible to pressure-induced strain unlike in bulk piezoelectric materials, where only the surface proximate volume generates a piezoelectric response when exposed to pressure differentials.

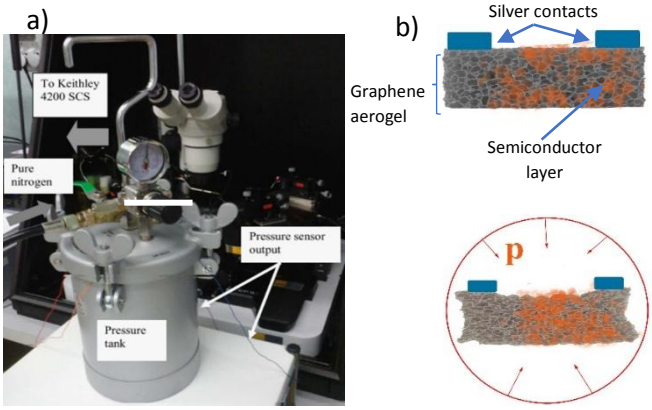

Fig. 3. a) Pressure testing chamber. b) Sensor structure before testing (top) and exposed to hydrostatic pressure (down).

The pressure sensor was built by contacting graphene aerogel/semiconductor samples with silver paste with further drying. The wires from the pressure sensor were connected to a Keithley 4200 SCS instrument with low noise amplifiers at outputs, and the electrical characterization was performed at room temperature at different pressures in a pressure tank, which is calibrated to increase the pressure from 1 to 5 atm by pumping pure nitrogen inside. Figure 4 displays the resistance–pressure dependence of bare aerogel at different pressure values and the same dependences for graphene aerogel decorated with semiconductor nanocrystalline layers. As can be observed, pure aerogel device the same as hybrid structures display resistance change. However, hybrid structures show improved linearity in the wide pressure range [11]. Pressure sensor sensitivity was defined 5 V of 5.6×10^{-4} kPa^{-1} for the aerogel–SnO_2 nanocomposite with 250 nm thickness and 6.7×10^{-4} kPa^{-1} with 350 nm, 6.75×10^{-4} kPa^{-1} for aerogel-GaN nanocomposite with 250 nm semiconductor layer, in case of 250nm CdS this value was calculated as 3.2 $10\times^{-4}$ kPa^{-1}.

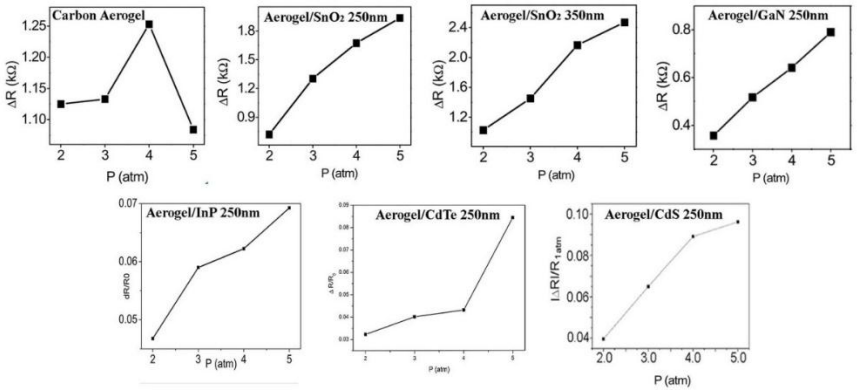

Fig. 4. Electro-mechanical characteristics of graphene aerogel/semiconductor pressure sensors.

Comparing proposed aerogel-semiconductor pressure sensors one can evidentiate higher linearity of aerogel/SnO2, GaN, CdS structures, resistance change for these structures is directly proportional to applied pressure. At forward-backward sensor cycling can also be attested hysteresys which can be reduced by increase of delays between application of pressure and collection of electrical signal.

Conclusions

Miniaturized, integrated smart devices generate an inevitable trend in the development of technology, which requires researches on combination of further sensors with integrated circuits. Although abundant ultra-sensitive sensors have been reported, new types of materials and sensing mechanisms still should be continuously optimized to meet the increasingly demanding application requirements. Moreover, emerging healthcare technologies such as real-time human health monitoring and clinical medicine require intelligent sensors for higher quality service. This work demonstrate that integration of piezoelectric semiconductor nanocrystals with flexible graphene aerogel contribute to the development of high efficient pressure sensitive devices, which have a great applicative potential at industrial, medical and household level.

References

1. M. Mecklenburg, A. Schuchardt, Y. K. Mishra, S. Kaps, R. Adelung, A. Lotnyk, L. Kienle, and K. Schulte, Aerographite: Adv. Mater. 2012, DOI: 10.1002/adma.201200491.
2. H. Sun, Z. Xu, and C. Gao, Adv. Mater. 25, 2013, 2554-2560.
3. Meng Wang, Changyou Shao, Sukun Zhou, Jun Yang, Feng Xu, Cellulose 2018.
4. He, J.; Nuzzo, R.G.; Rogers, J.A. Proc. IEEE 2015, 103, 619–632.
5. Oh, J.Y.; Rondeau-Gagné, S.; Chiu, Y.C.; Chortos, A.; Lissel, F.; Wang, G.N.; Schroeder, B.C.; Kurosawa, T.; Lopez, J.; Katsumata, T. Nature 2016, 539, 411.
6. Chen, X. Making Electrodes Stretchable. Small Methods 2017, 1, 1600029.
7. Jonghwa, P.; Youngoh, L.; Jaehyung, H.; Minjeong, H.; Young-Do, J.; Hyuneui, L.; Sung Youb, K.; Hyunhyub, K. ACS Nano 2014, 8, 4689–4697.
8. Pan, L.; Chortos, A.; Yu, G.; Wang, Y.; Isaacson, S.; Allen, R.; Shi, Y.; Dauskardt, R.; Bao, Z. Nat. Commun. 2014, 5, 3002.
9. Ruo-Zhou, L.; Anming, H.; Tong, Z.; Oakes, K.D. ACS Appl. Mater. Interfaces 2014, 6, 21721–21729.
10. Woo, S.J.; Kong, J.H.; Kim, D.G.; Kim, J.M. J. Mater. Chem. C 2014, 2, 4415–4422.
11. Dragoman, M.; Ghimpu, L.; Obreja, C.; Dinescu,A.; Plesco, I.; Dragoman, D.; Braniste, T.; Tiginyanu, I., Nanotechnology 27 (2016) 475203.
12. Plesco, I.; Dragoman, M.; Strobel, J.; Ghimpu, L.; Schütt, F.; Dinescu, A.; Ursaki, V.; Kienle, L.; Adelung, R.; Tiginyanu, I., Superlattices and Microstructures 117 (2018) 418-422.
13. Liu, Y.; Tao, L.-Q.; Wang, D.-Y.; Zhang, T.-Y.; Yang, Y.; Ren, T.-L. Appl. Phys. Lett. 2017, 110, 123508.
14. Samad, Y.A.; Li, Y.; Schiffer, A.; Alhassan, S.M.; Liao, K. Small 2015, 11, 2380–2385.
15. He, Y.; Li, W.; Yang, G.; Liu, H.; Lu, J.; Zheng, T.; Li, X. Materials 2017, 10, 684.
16. Chwee-Lin, C.; Mun-Bo, S.; Byoung-Sun, L.; Sanghun, J.; Dong-Su, K.; Tae-Hyung, K.; Jihyun, B.; Sung Hoon, L.; Kyung-Eun, B.; Jungkyun, I. Adv. Mater. 2014, 26, 3451–3458.
17. Smith A D et al 2013, Nano Lett. 13, 3237–43.
18. Zewei Luo, Xiaotong Hu, Xiyue Tian, Chen Luo, Hejun Xu, Quanling Li, Qianhao Li, Jian Zhang, Fei Qiao, Xing Wu, V. E. Borisenko and Junhao Chu, Sensors 2019, 19, 1250.
19. Pyo, S.; Choi, J.; Kim, J. Adv. Electron. Mater. 2018, 4, 1700427.
20. Cataldi, P.; Dussoni, S.; Ceseracciu, L.; Maggiali, M.; Natale, L.; Metta, G.; Athanassiou, A.; Bayer, I.S. Adv. Sci. 2018, 5, 1700587.
21. Mitrakos, V.; Macintyre, L.; Denison, F.; Hands, P.; Desmulliez, M. Design, Micromachines 2017, 8, 41.
22. Nie, B.; Li, R.; Cao, J.; Brandt, J.D.; Pan, T. Adv. Mater. 2015, 27, 6055–6062.
23. Chen, S.; Jiang, K.; Lou, Z.; Chen, D.; Shen, G. Adv. Mater. Technol. 2018, 3, 1700248.
24. He, Z.; Chen, W.; Liang, B.; Liu, C.; Yang, L.; Lu, D.; Mo, Z.; Zhu, H.; Tang, Z.; Gui, X. ACS Appl. Mater. Interfaces 2018, 10, 12816–12823.
25. Choi, T.; Hwang, B.U.; Kim, B.Y.; Trung, T.Q.; Nam, Y.H.; Kim, D.N.; Eom, K.; Lee, N.E. ACS Appl. Mater. Interfaces 2017, 9, 18022–18030.
26. Ho, D.H.; Sun, Q.; Kim, S.Y.; Han, J.T.; Kim, D.H.; Cho, J.H. Adv. Mater. 2016, 28, 2601–2608.
27. Amjadi, M.; Kyung, K.U.; Park, I.; Sitti, M. Adv. Funct. Mater. 2016, 26, 1678–1698.